Structural Analysis of d(GCAATTGC)$_2$ and Its Complex with Berenil by Nuclear Magnetic Resonance Spectroscopy†

Mitsuru Yoshida, Debra L. Banville, and Richard H. Shafer*

Department of Pharmaceutical Chemistry, School of Pharmacy, University of California, San Francisco, California 94143

Received October 11, 1989; Revised Manuscript Received February 26, 1990

ABSTRACT: The structures of d(GCAATTGC)$_2$ and its complex with berenil in solution were analyzed by two-dimensional ^{1}H NMR spectroscopy. Intra- and internucleotide nuclear Overhauser effect (NOE) connectivities demonstrate that the octanucleotide duplex is primarily in the B conformation. Binding with berenil stabilizes the duplex with respect to thermal denaturation by about 10 °C, based on the appearance of the imino proton signals. The berenil–d(GCAATTGC)$_2$ system is in fast exchange on the NMR time scale. The two-dimensional NMR data reveal that berenil binds in the minor groove of d(GCAATTGC)$_2$. The aromatic drug protons are placed within 5 Å of the H2 proton of both adenines, the H1′, H5′, and H5″ of both thymidines, and the H4′, H5′, and H5″ of the internal guanosine. The amidine protons on berenil are also close to the H2 proton of both adenines. The duplex retains an overall B conformation in the complex with berenil. At 18 °C, NOE contacts at longer mixing times indicate the presence of end-to-end association both in the duplex alone and also in its complex with berenil. These intermolecular contacts either vanished or diminished substantially at 45 °C. Two molecular models are proposed for the berenil–(GCAATTGC)$_2$ complex; one has hydrogen bonds between the berenil amidine protons and the carbonyl oxygen, O2, of the external thymines, and the other has hydrogen bonds between the drug amidine protons and the purine nitrogen, N3, of the internal adenines. Quantitative analysis of the NOE data favors the second model.

Berenil [4,4′-(1-triazene-1,3-diyl)bis(benzamidine), Figure 1], a trypanosidal drug, is classified as a diarylamidine compound which binds to double-helical DNA. The binding of berenil to DNA shifts the absorption maximum of the drug from 370 to 380 nm (Newton, 1967) but does not cause unwinding of closed circular DNA (Waring, 1970), suggesting that its mode of binding is not intercalative. It is probable that berenil binds, like netropsin and distamycin, in the minor groove of duplex DNA (Kopka et al., 1985a,b). One berenil molecule has been reported to bind to 4 base pairs (Waring, 1970; Braithwaite & Baguley, 1980), and preference for A-T sequences over G-C sequences has been observed (Braithwaite & Baguley, 1980; Portugal & Waring, 1987).

Molecular modeling studies of the berenil–DNA complex have been carried out by Gresh and Pullman (1984) and Pearl et al. (1987). Gresh and Pullman, who used the B-form d-(AT)$_n$·d(AT)$_n$ double helix as a DNA model, reported that berenil interacts in the minor groove, where two hydrogen bonds are formed between the amidine groups of the drug and the oxygen atoms of the thymines in adjacent AT pairs. Pearl et al. determined the crystal structure of berenil and used these coordinates to model its interaction with DNA. Their model assumed the same drug–DNA hydrogen bonds as Gresh and Pullman reported for the d(AT)$_4$·d(AT)$_4$ sequence. In addition, they described the formation of hydrogen bonds between berenil and the N3 atoms of the diad-related central adenines for the d(TA)$_4$·d(TA)$_4$ oligomer, as well as asymmetric hydrogen bonds, one on thymine O2 and the other on adenine N3, for the complex with dA$_2$·dT$_8$. Following energy minimization, however, these hydrogen bonds either diminished in strength or disappeared. Pearl et al. (1987) described this as a possible artifact due to the theoretical treatment of phosphate negative charges. A crystal structure of a berenil–DNA complex itself, however, has not yet been reported.

In this work, we have obtained models for the solution structure of both d(GCAATTGC)$_2$ and its complex with berenil via two-dimensional (2-D)[1] ^{1}H NMR spectroscopy.

Materials and Methods

Berenil diaceturate was purchased from Sigma (St. Louis, MO), and d(GCAATTGC) was from Pharmacia P-L Biochemicals (Milwaukee, WI). The concentration of solutions of the oligonucleotide was determined by measuring the absorbance at 260 nm in buffer containing 1 M NaCl and assuming an extinction coefficient (ϵ) of 105 600 mol^{-1} cm^{-1} for duplex d(GCAATTGC)$_2$. The ϵ for berenil at 370 nm is 34 400 mol^{-1} cm^{-1} in sodium phosphate buffer [20 mM phosphate, 100 mM NaCl, and 50 μM EDTA (pH 7.0)]. The berenil–d(GCAATTGC)$_2$ complex for 2-D ^{1}H NMR analysis consisted of d(GCAATTGC) (8.6 mM) and berenil diaceturate (4.3 mM) in sodium phosphate buffer [20 mM phosphate, 100 mM NaCl, and 50 μM EDTA (pH 7.0)]. Comparison of NMR intensities confirmed the 2:1 ratio of oligonucleotide strand to drug.

All ^{1}H NMR spectra were measured at 18 °C on a GN-500 spectrometer (General Electric, Fremont, CA) at a proton

† Supported by USPHS Grant CA 27343 awarded by the National Cancer Institute, DHHS, and a scholarship from the Science and Technology Agency of Japan. The computer Graphics Laboratory at UCSF is supported by Grant RR-01081 from the Division of Research Resources, NIH, DHHS.

* To whom correspondence should be addressed.

[1] Abbreviations: COSY, ^{1}H two-dimensional *J*-correlation NMR spectroscopy; DNA, deoxyribonucleic acid; EDTA, ethylenediaminetetraacetic acid; FID, free induction decay; HOHAHA, homonuclear Hartmann–Hahn relayed spectroscopy; NMR, nuclear magnetic resonance; NOE, nuclear Overhauser enhancement; NOESY, ^{1}H two-dimensional NOE correlation NMR spectroscopy in the pure absorption mode; 1-D, one dimensional; 2-D, two dimensional; CORMA, complete relaxation matrix analysis.

0006-2960/90/0429-6585$02.50/0

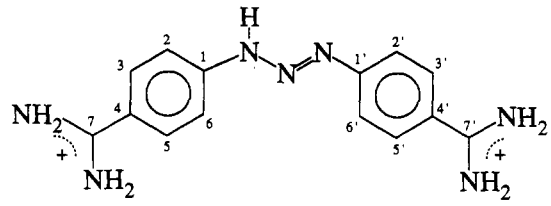

FIGURE 1: Structure of berenil.

frequency of 500.0 MHz. One-dimensional ^{1}H NMR spectra of the low-field region (12.5–14.2 ppm), which contains the imino protons, were obtained with a $1\bar{3}3\bar{1}$ pulse sequence (Hore, 1983). The 2-D spectra were processed on a Sun/AT&T System 4 computer. The NOESY, $1\bar{3}3\bar{1}$ pulse NOESY, and HOHAHA spectra were implemented with 2K data points in the t_2 dimension and 400 data points of 16 FID's each in the t_1 dimension. NOESY experiments were carried out with repetition times of 3 s. For double quantum filtered COSY experiments, 800 data points were used in the t_1 dimension. The FID's were zero-filled once and apodized with Gaussian window functions in both dimensions.

The berenil–d(GCAATTGC)$_2$ model was displayed with the molecular interactive graphics program MIDAS (Ferrin & Langridge, 1980; Langridge et al., 1981). The initial coordinates for berenil were obtained from its energy-minimized structure (S. Neidle, personal communication) based on the crystal structure data (Pearl et al., 1987). The coordinates for carbons, nitrogens, and oxygens in the B-form oligonucleotide were calculated by the program NUCGEN (written by U. C. Singh, N. Pattabiraman, and S. Rao, University of California at San Francisco, in 1986) based on data files of the crystal structures of Arnott B–DNA duplexes, and hydrogens were added by using standard bond lengths and bond angles.

Complete relaxation matrix analysis (CORMA) was used to compare the observed berenil-to-DNA cross-peak intensities with those predicted for the two models discussed below (Keeper & James, 1984). The proton T_1 values of the drug–DNA complex were sufficiently short, presumably due to the intermolecular contacts, so that repetition times of 3 s were appropriate for measurement of cross-peak intensities needed for the CORMA calculations. A correlation time of 7 ns was used in this analysis. Values between 1 and 5 ns did not have a significant effect upon the calculated intensities. Each model was compared with the experimental data by determining the root mean square (RMS) value of the differences between the observed and calculated intensities for the berenil–oligonucleotide complex.

Results and Discussion

The oligonucleotide studied, d(GCAATTGC)$_2$, is self-complementary and has 2-fold symmetry. Its central four AT base pairs were presumed to be a binding site of berenil, on the basis of earlier studies (Braithwaite & Baguley; Portugal & Waring, 1987). In addition, two GC base pairs are attached on the ends to stabilize the duplex structure.

Two-Dimensional ^{1}H NMR Analysis of d(GCAATTGC)$_2$. The assignments of the nonexchangeable protons of d(GCAATTGC)$_2$ were achieved by analyzing NOESY data (mixing times of 50, 150, 250, and 400 ms), along with double quantum filtered COSY data and HOHAHA data (mixing time of 70 ms). The results are shown in Table I. The H1′, H2′, H2″, H3′, and base protons were assigned sequentially by using the internucleotide NOE connectivity through the base H8 and H6 protons. Most of the NOE contacts between the base protons and the 5′-linked sugar H1′, H2′, H2″, and

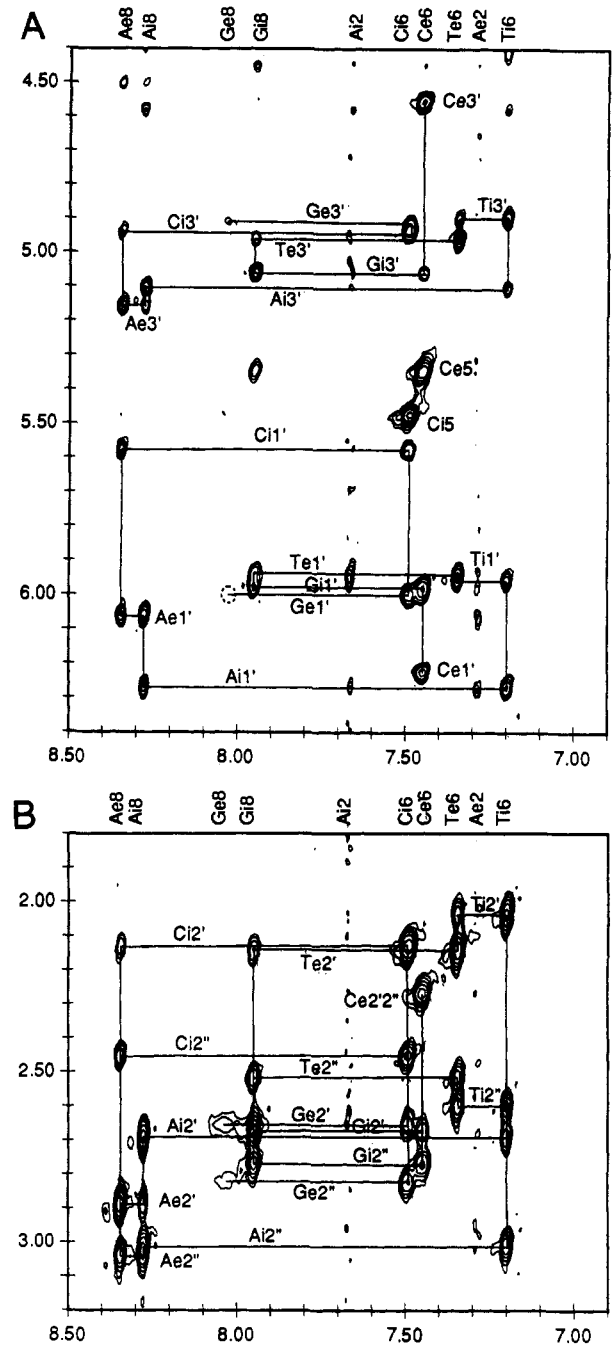

FIGURE 2: Base proton–H1′, H3′ region (A) and base proton–H2′, H2″ region (B) in the NOESY spectrum of d(GCAATTGC)$_2$ at a 150-ms mixing time. The lower case letters e and i refer to the external and internal residues, respectively. The lines trace the sequential assignments of the base protons and the deoxyribose H1′, H2′, H2″, and H3′ protons.

H3′ are clearly observed at a mixing time of 150 ms, suggesting that the duplex is in a right-handed conformation with deoxyribonucleosides in the anti conformation (Figure 2A,B). The contact of the 5′-terminal guanine H8 to H1′ of its own sugar is not observed at this mixing time (Figure 2A), although this contact did appear weakly in the longer mixing time experiments. This may be due to the motion of the terminal nucleoside, which is confirmed by the fact that the imino proton in the terminal GC base pair is broadened under partial exchange with the solvent water proton (Figure 5A). Since the intranucleotide contacts of base protons with H1′ and H2″ are stronger than those with H3′ (Figure 2A,B), the oligonucleotide is presumed to be in an overall B-type conformation characterized by C2′-endo sugar pucker (Wuthrich, 1986).

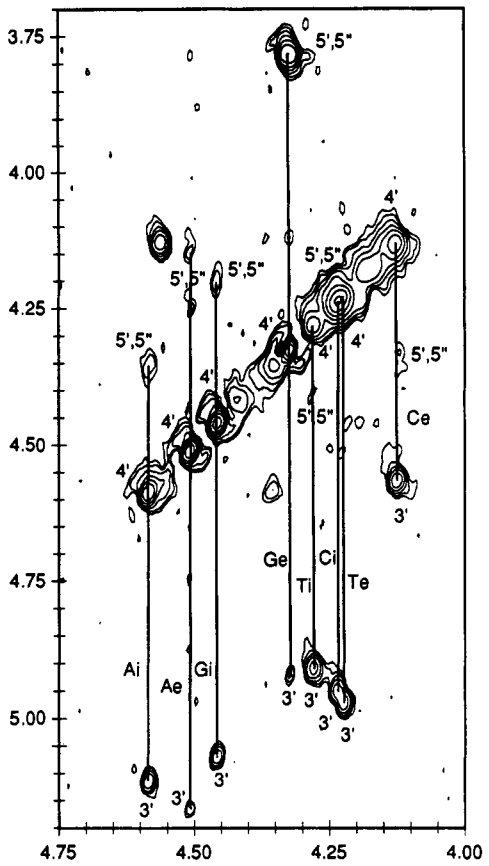

FIGURE 3: H4′–H3′, H5′/H5″ region in the HOHAHA spectrum of d(GCAATTGC)$_2$ at a 70-ms mixing time. The assignments of all H4′ protons can be made from H3′–H4′ cross-peaks. The assignments of H5′/H5″ protons which are made from NOESY spectra are confirmed by H4′–H5′/H5″ cross-peaks (see text).

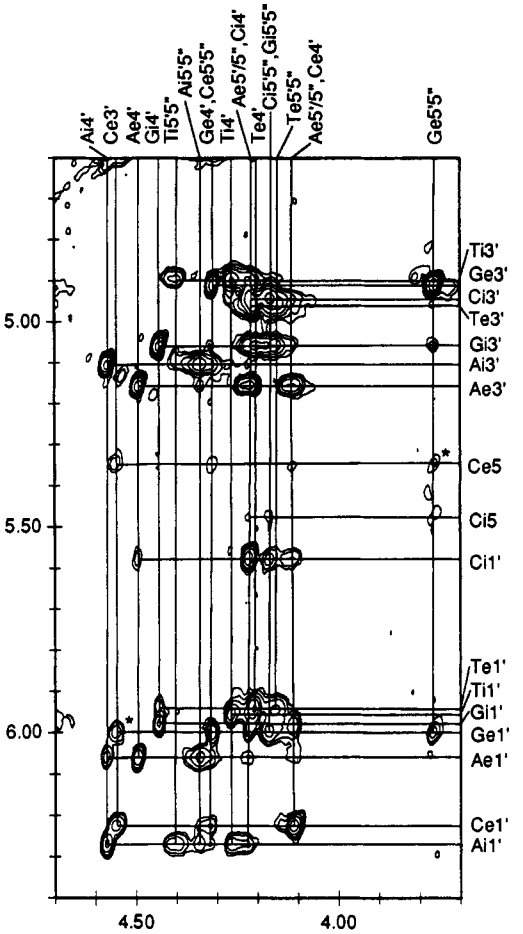

FIGURE 4: H1′, H3′–H4′, H5′/5″ region in the NOESY spectrum of d(GCAATTGC)$_2$ at a 250-ms mixing time. The assignments of H5′/H5″ protons are made in this region after H4′ protons are assigned by the COSY and HOHAHA experiments. The cross-peaks indicated by an asterisk are derived from an end-to-end association of two duplexes (see text).

The adenine H2 protons were assigned from NOE contacts with their own sugar H1′, the 3′-linked H1′, and the H1′ of their complementary base-paired thymine on the opposite strand at mixing times of 250 and 400 ms. The interaction between adenine H2 and thymidine H1′ of each central base pair provides further evidence for a right-handed conformation of the duplex. In addition, the NOE cross-peaks between the H2 protons of the two adjacent adenines were observed at a mixing time of 150 ms.

The signals in the crowded 4.0–4.6 ppm region contain the H4′, H5′, and H5″ resonances and were assigned as follows: First, the H4′ signals were assigned from their H3′–H4′ coupling observed in the COSY and HOHAHA spectra (Figure 3). Second, the H5′/H5″ signals were assigned from their intranucleotide contacts with H1′, H2, H2″, and H3′ in the NOESY spectra at mixing times of 250 ms (Figure 4) and 400 ms. These assignments were confirmed by H4′–H5′/H5″ cross-peaks in the HOHAHA spectrum (Figure 3). Differentiation between the H5′ and H5″ protons was possible for one of the nucleotides, where the chemical shifts of these protons differed by more than 0.03 ppm and no other NOE cross-peaks overlapped with these base proton to H5′ and H5″ cross-peaks (Table I). The base proton in a nucleotide in B-DNA is closer to its own H5′ proton than to its H5″ proton, so that the base proton–H5′ cross-peak should be stronger than the base proton–H5″ cross-peak in a NOESY spectrum at short mixing times.

The cytosine NH_2 protons were observed in the $1\bar{3}3\bar{1}$ pulse NOESY spectrum in 90% H_2O/10% D_2O at a 250-ms mixing time and assigned from their contacts with their own H5 protons. The NH protons of the guanines and thymines were assigned on the basis of NOE contacts across the base pair with cytosine NH_2 and adenine H2 protons. The NH_2 protons of adenines and guanines were not observed.

In addition to the intraduplex NOE contacts described above, several interduplex contacts were found in the NOESY spectra at mixing times of 150 ms or longer. These contacts were end-to-end contacts from the terminal guanosine H1′ to the terminal cytidine H2′/H2″ and H3′, and from the terminal guanosine H5′/H5″ to the terminal cytidine H5, H6, and H3′. A similar association of the ends between the duplexes has been reported by Genest et al. (1987) for the Z form of d(br^{5}C-G)$_3$.

Imino Proton Region of the Berenil–d(GCAATTGC)$_2$ Complex in 1-D NMR. Berenil was titrated into a solution of d(GCAATTGC)$_2$ to investigate the formation of the drug–oligonucleotide complex by 1-D ^{1}H NMR spectroscopy. The imino proton region of d(GCAATTGC)$_2$ is shown in Figure 5 as a function of increasing berenil concentration. In the absence of berenil, the imino proton region consists of four signals corresponding to guanine and thymine (Figure 5A). Throughout the titration, the number of imino proton signals does not change; however, their chemical shifts are altered significantly (Figure 5B–D). Distinct signals for drug-free DNA and drug-bound DNA are not detected. Similar changes were noted in the aromatic region, and this indicated that the berenil–oligonucleotide system is in fast exchange on the NMR time scale. Fast exchange was observed even at temperatures as low as 2 °C. Binding of berenil brought about a large downfield shift of the internal thymine imino proton and a

Table I: Assignments (ppm) of ^{1}H NMR Signals

	−berenil	+berenil	shift		−berenil	+berenil	shift
Ge H8	8.07	7.92	−0.15	Ge H3′	4.91	4.85	−0.06
Ci H5	5.47	5.41	−0.06	Ci H3′	4.94	4.89	−0.05
Ci H6	7.49	7.42	−0.07	Ae H3′	5.15	5.12	−0.03
Ae H2	7.29	7.22	−0.07	Ai H3′	5.10	5.03	−0.07
Ae H8	8.35	8.32	−0.03	Ti H3′	4.90	4.60	−0.30
Ai H2	7.67	8.08	0.41	Te H3′	4.96	4.66	−0.30
Ai H8	8.28	8.22	−0.06	Gi H3′	5.05	4.97	−0.08
Ti H6	7.20	6.96	−0.24	Ce H3′	4.55	4.51	−0.04
Ti CH_3	1.38	1.28	−0.10	Ge H4′	4.32	4.25	−0.07
Te H6	7.35	7.05	−0.30	Ci H4′	4.23	4.18	−0.05
Te CH_3	1.66	1.51	−0.15	Ae H4′	4.50	4.48	−0.02
Gi H8	7.95	7.77	−0.18	Ai H4′	4.58	4.44	−0.14
Ce H5	5.34	5.22	−0.12	Ti H4′	4.27	2.77	−1.50
Ce H6	7.45	7.34	−0.11	Te H4′	4.21	3.23	−0.98
Ge H1′	6.00	5.91	−0.09	Gi H4′	4.45	4.29	−0.16
Ci H1′	5.57	5.50	−0.07	Ce H4′	4.12	4.07	−0.05
Ae H1′	6.06	6.02	−0.04	Ge H5′/5″	3.77	3.91	0.14
Ai H1′	6.26	6.18	−0.08	Ci H5′/5″	4.18	4.12	−0.06
Ti H1′	5.95	5.54	−0.41	Ae H5′/5″	4.12	4.09	−0.03
Te H1′	5.94	4.97	−0.97	Ae H5′/5″	4.24	4.19	−0.05
Gi H1′	5.98	5.84	−0.14	Ai H5′/5″	4.34	4.30	−0.04
Ce H1′	6.22	6.19	−0.03	Ti H5′/5″	4.40	3.90	−0.50
Ge H2′	2.65	2.58	−0.07	Ti H5′/5″	4.40	3.93	−0.47
Ci H2′	2.13	2.09	−0.04	Te H5′	4.16	3.90	−0.26
Ae H2′	2.88	2.87	−0.01	Te H5″	4.16	3.61	−0.55
Ai H2′	2.68	2.60	−0.08	Gi H5′	4.19	3.71	−0.48
Ti H2′	2.04	1.74	−0.30	Gi H5″	4.19	4.13	−0.06
Te H2′	2.14	1.82	−0.32	Ce H5′	4.32	4.25	−0.07
Gi H2′	2.67	2.51	−0.16	Ce H5″	4.36	4.10	−0.26
Ce H2′	2.27	2.21	−0.06	Ge NH	13.03	13.00	−0.03
Ge H2″	2.82	2.75	−0.07	Ci NH_2	6.44	6.44	0.00
Ci H2″	2.45	2.42	−0.03		8.47	8.46	−0.01
Ae H2″	3.04	3.00	−0.04	Ti NH	13.69	13.83	0.14
Ai H2″	3.02	2.84	−0.18	Te NH	13.85	13.80	−0.05
Ti H2″	2.60	2.24	−0.36	Gi NH	12.80	12.80	0.00
Te H2″	2.52	2.12	−0.40	Ce NH_2	6.65	6.60	−0.05
Gi H2″	2.76	2.67	−0.09		8.23	8.24	0.01
Ce H2″	2.27	2.21	−0.06				

	−DNA	+DNA	shift		−DNA	+DNA	shift
berenil H2	7.66	7.95	0.29	berenil amidine	8.03	8.79	0.76
berenil H3	7.83	8.20	0.37			8.87	0.84

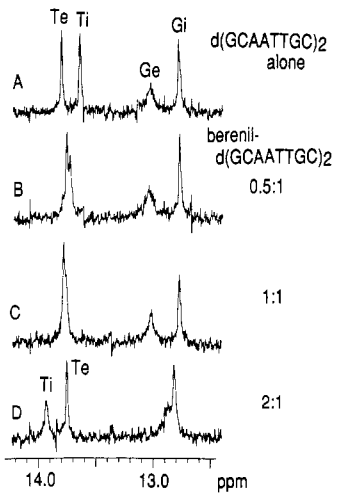

FIGURE 5: Spectral changes in the imino proton region of d-(GCAATTGC)$_2$ observed with increasing concentrations of berenil. The duplex (0.23 mM) was in 25% D_2O/sodium phosphate buffer [20 mM phosphate, 100 mM NaCl, and 50 μM EDTA (pH 7.0)], and the spectra were collected in 40 scans over a spectral width of 12000 Hz by a $1\bar{3}3\bar{1}$ pulse sequence. The four imino protons are assigned for the drug-free duplex as indicated in the figure, where e and i refer to the external and internal residues, respectively.

smaller upfield shift of the external thymine imino proton. This observation is consistent with drug binding at the A-T base pair region of the oligonucleotide. The shifts of the G-C imino protons observed at the high ratio of berenil to DNA (Figure 4D) are considered to be derived from a secondary, nonspecific mode of binding. This type of binding was first seen in UV studies, where a second isosbestic point was observed at high ratios of berenil to DNA in titrations using poly(dA-dT)·poly(dA-dT) and poly(dA)·poly(dT) (data not shown). Similar biphasic changes in the absorption spectrum have been reported for other nonintercalative drugs such as DDUG and SN 6999 (Braithwaite & Baguley, 1980).

Binding of berenil stabilized the duplex against heat denaturation (data not shown). The signals of the nonterminal imino protons in the duplex alone were broad at 45 °C and unobservable at 50 °C due to the dissociation of the strands. At a 1:1 stoichiometry, however, the imino proton signals did not appear to broaden significantly until 55 °C, and they disappeared at 60 °C. This result indicates that the central part of the duplex is protected from thermal denaturation by the drug.

Two-Dimensional ^{1}H NMR Analysis of the Berenil–d-(GCAATTGC)$_2$ Complex. In NOESY experiments, cross-peaks result from the exchange of magnetization through dipole–dipole cross-relaxation. Consider a spin system undergoing chemical exchange, such as a biopolymer–ligand complex in which molecules exchange between free and bound forms. When exchange is fast on the cross-relaxation rate time scale, the sum of the bound and free magnetization decays through the equilibrium–concentration–weighted sum of the

bound and free relaxation and transferred nuclear Overhauser enhancements (TRNOE) can be observed (Landy & Rao, 1989). If the observed signals from two components are indistinguishable, only their sum can be measured. Landy and Rao demonstrated the following equation for the fast-exchange n-spin system:

$$d(\mathbf{m}_b + \mathbf{m}_f)/dt = (p_b\mathbf{W}_b + p_f\mathbf{W}_f)(\mathbf{m}_b + \mathbf{m}_f)$$

where b and f refer to the bound and free species, respectively, p_b and p_f are the fractional concentrations of the bound and free species, respectively, and $\mathbf{W}$ is the $n \times n$ relaxation matrix. The elements, m_i, of the n-component vector, $\mathbf{m}$, are given by

$$m_i = M_{zi} - M_{0i}$$

in which M_{zi} is the instantaneous value of the z component of magnetization of spin i and M_{0i} is its equilibrium value.

Since the binding constants of berenil for poly(dA-dT)·poly(dA-dT) and poly(dA)·poly(dT) are on the order of 10^4–10^5 M^{-1} (unpublished data), it can be assumed that the equilibrium for berenil binding to d(GCAATTGC)$_2$ lies far to the bound state at NMR concentrations, that is, $p_f \approx 0$, $p_b \approx 1$. Then the equation above becomes

$$d(\mathbf{m}_b + \mathbf{m}_f)/dt = \mathbf{W}_b(\mathbf{m}_b + \mathbf{m}_f)$$

Hence, the rate equation is dependent only on the bound-state rate matrix, and we can detect NOE effects as if we were looking at a stable complex without complications due to exchange with the free state.

The signal assignments of the berenil–d(GCAATTGC)$_2$ complex were made by the same strategy described for the oligonucleotide alone (Table I). The NOE contacts between the base protons and the 5′-linked H1′, H2′, H2″, and H3′ sugar protons are still observed between each nucleotide, showing that the B conformation of the duplex is retained in the complex with berenil (Figure 6A). Furthermore, the 2-fold symmetry of the oligonucleotide is retained in the berenil complex, where only one set of drug and DNA resonances is observed (Figure 6A,B).

We investigated the relative changes in the NOE peak volumes of base proton contacts to their own sugar H1′, H2′, and H2″ for the drug complex. Changes in the helical twist or base stacking will be reflected in these intranucleotide NOE cross-peaks intensities and their relative chemical shifts. No obvious changes were observed for the external adenosine, the internal thymidine, or the internal guanosine cross-peaks at mixing times of 150 and 250 ms. Interestingly, the external thymidine H1′ signal exhibited a large upfield shift (0.97 ppm) upon complex formation. Unfortunately, the external thymidine base–H1′ cross-peak of the duplex alone overlaps with the internucleotide cross-peak between the external thymidine base proton and the internal thymidine H1′ proton (Figure 2A). The internal adenosine H8–H2″ cross-peak also overlaps with the internucleotide contact peak between the internal adenosine H8 and the external adenosine H2″ in both duplex alone (Figure 2B) and complex. Moreover, in the complex, the internal adenosine H8–H1′ cross-peak overlaps with the internal adenosine H1′–berenil H3 cross-peak (Figure 6A). Therefore, we could not determine the relative NOE intensities associated with these proton pairs. For the resolvable NOE cross-peaks, however, there was no significant change in base–sugar H1′, H2′, and H2″ distances elicited by drug complexation.

The signals of the berenil aromatic protons are observed as two broad peaks at 7.95 and 8.20 ppm (Figure 6B). The peak at 8.20 ppm was assigned to H3 of berenil from the strong cross-peaks with the amidine protons in the $1\bar{3}3\bar{1}$ NOESY experiment (Figure 8), and the peak at 7.95 ppm was assigned to berenil H2. It was impossible to distinguish the signals of berenil H2 and H3 from those of H6 and H5. The overlap of the chemical shift of these protons could be due to rapid flipping of the aromatic rings, which could lead to line broadening as well.

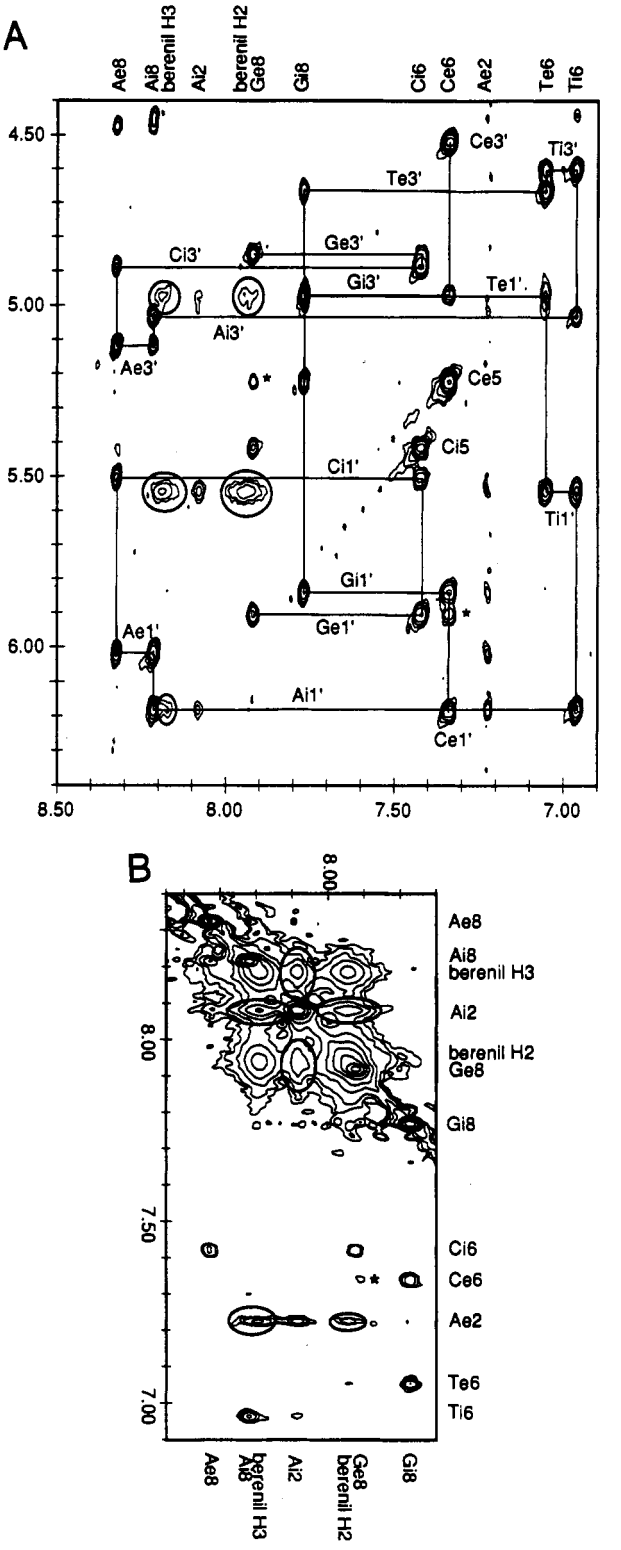

FIGURE 6: Aromatic proton–H1′,H3′ region (A) and aromatic proton region (B) in the NOESY spectrum of the berenil–d(GCAATTGC)$_2$ complex at a 150-ms mixing time. The lower case letters e and i refer to the external and internal residues, respectively. The lines trace the sequential assignments of the base protons and the deoxyribose H1′ and H3′ protons. Circled cross-peaks are the contacts between berenil and d(GCAATTGC)$_2$, and the cross-peaks indicated by an asterisk are derived from an end-to-end association of two duplexes (see text).

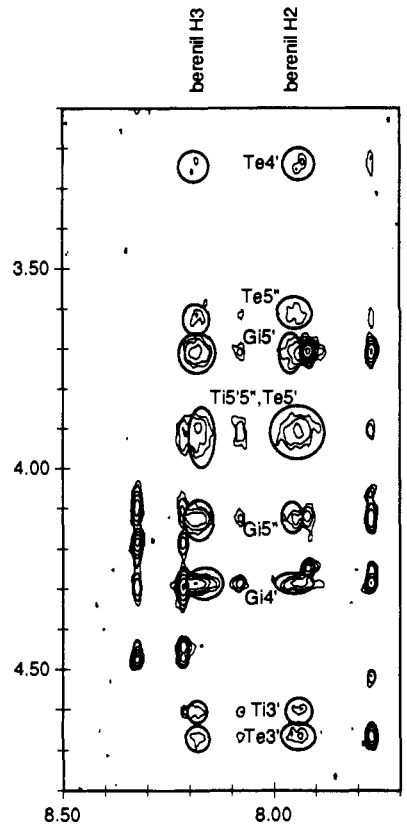

FIGURE 7: NOE contacts between berenil aromatic protons and H3′, H4′, and H5′/H5″ protons of d(GCAATTGC)$_2$ at a 400-ms mixing time. The lower case letters e and i refer to the external and internal residues, respectively. Circled cross-peaks are the contacts between berenil and d(GCAATTGC)$_2$.

The berenil–d(GCAATTGC)$_2$ intermolecular contacts observed in the NOESY experiments are listed in Table II. The NOESY spectrum with a 150-ms mixing time shows obvious contacts from the berenil aromatic protons to both adenine H2 protons (Figure 6B), both thymine H1′ protons (Figure 6A), the H5′/H5″ of the internal thymidine and/or H5′ of the external thymidine proton, and the H4′ and H5′ of the internal guanosine protons. More specifically, the berenil H3 proton has contacts with H1′ of the internal adenosine (Figure 6A) and H5″ of the internal guanosine in addition. At mixing times of 250 and 400 ms (Figure 7), berenil H2 has obvious contacts with H1′ of the internal adenosine, H4′ and H5″ of the external thymidine, and H5″ of the internal guanosine. Weak NOE contacts of the berenil aromatic protons to H2″ of the internal thymidine, H6 and H3′ of both thymidines, and H8 of the internal guanosine were also observed at mixing times of 250 and 400 ms. These weak drug contacts to protons situated in the DNA major groove most likely arise from secondary NOE effects.

The H1′ and H4′ signals of the external thymidine and H4′ of the internal thymidine were shifted significantly upfield (1–1.5 ppm) by complex formation, and substantial upfield shifts (0.3–0.5 ppm) were also observed for the other protons of the two thymidines (Table I). On the other hand, the H2 of the internal adenine shifted 0.4 ppm downfield (Table I). These shifts could be caused by ring current effects of the berenil aromatic rings.

A NOESY experiment in 90% H_2O/10% D_2O at 250-ms mixing time using the $1\bar{3}3\bar{1}$ pulse was performed to observe the exchangeable protons. It shows contacts between the berenil amidine protons and the adenine H2 protons (Figure 8). The diazoamino proton of berenil is not detected, and this is probably because of fast exchange with solvent.

Table II: NOE Contacts between Berenil and d(GCAATTGC)$_2$ Protons

	NOE[a] for berenil	
	H2	H3
Ae H2	+++	++++
Ai H2	++++	++++
Ti H6	++	++
Ti CH_3	–	++
Te H6	++	++
Te CH_3	+	++
Gi H8	++	++
Ai H1′	+++	+++
Ti H1′	++++	++++
Te H1′	+++	+++
Gi H1′	+	++
Ti H2′	–	+
Ti H2″	+	+
Ti H3′	++	++
Te H3′	++	++
Gi H3′	–	+
Te H4′	+++	+
Gi H4′	+++	++++
Ti H5′/H5″/Te H5′	+++	+++
Te H5″	+++	++
Gi H5′		+++
Gi H5″	+++	+++

[a] (++++) Observed at a mixing time of 50 ms or longer; (+++) 150 ms or longer; (++) 250 ms or longer; (+) 400 ms; (–) no cross-peak at a mixing time of 400 ms or less.

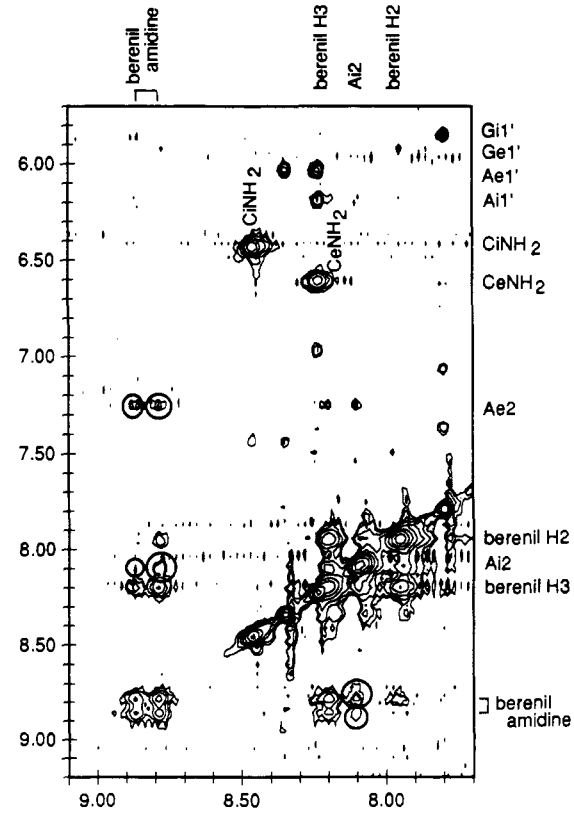

FIGURE 8: Base proton and H1′ region in the $1\bar{3}3\bar{1}$ pulse NOESY spectrum of the berenil–d(GCAATTGC)$_2$ complex at 250-ms mixing time. Circled cross-peaks are the contacts between berenil and d-(GCAATTGC)$_2$.

For berenil alone, a single resonance is observed for the amidine protons. In contrast, for bound berenil, two signals were assigned to the amidine protons: the one observed at higher field was assigned to the NH_2 group facing into the minor groove based on the stronger NOE contacts with the

adenine H2 protons, and the other was assigned to the NH_2 group pointing outside of the groove. The difference in the chemical shift of the two amidine signals is 0.08 ppm; therefore, any exchange between these two NH_2 groups must have a rate less than 90 s^{-1} according to the equation $^{n}k_{ex} = \pi(\Delta\nu)/\sqrt{2}$, where k_{ex} is the exchange rate at the coalescence point and $\Delta\nu$ is the chemical shift difference in frequency (Sanders & Hunter, 1988).

Unlike berenil, the asymmetric minor groove binders netropsin (Patel & Shapiro, 1986), distamycin (Klevit et al., 1986), and SN6999 (Leupin et al., 1986) removed the 2-fold symmetry of the oligomers studied and revealed that these drugs undergo flip-flop motions between two binding sites. This was evidenced by proton exchange peaks between the two chemically inequivalent DNA strands. The 2-fold symmetry of berenil and its complex with d(GCAATTGC)$_2$ makes it impossible to detect similar exchange peaks and hence to determine unequivocally if such flip-flop motion occurs. However, the equivalence of protons H2 and H3 with H5 and H6 suggests that the phenyl ring undergoes rotational motion.

Evidence for end-to-end association of the duplex was also detected for this complex, as well as the duplex alone. The resonance of the terminal guanosine H8 was sharper, and the guanosine H1′ was more isolated from other signals in the complex than in the duplex alone. Thus, more NOE cross-peaks between the 5′-terminal guanosine and the 3′-terminal cytidine could be assigned. The following contacts between the terminal guanosine and terminal cytosine residues suggested that the duplexes were associated via end-to-end stacking: GH8 to CH5, CH6, CH1′, and CH2′/2″; GH1′ to CH5, CH6, CH2′/2″, CH3′, and CH4′; and the GH5′/5″ to CH5, CH6, and CH3′. The cross-peaks derived from this end-to-end association diminished substantially or disappeared by 45 °C.

Modeling of the Berenil–d(GCAATTGC)$_2$ Complex. Since NOE contacts are usually observed when two protons lay within approximately 5 Å of each other, we hand-docked berenil with d(GCAATTGC)$_2$ in the B conformation according to the NOE contacts observed in our NOESY experiments. We obtained two possible models, which can explain all of the drug–DNA contacts. Model I has hydrogen bonds between berenil amidine protons and O2 of the external thymines (Figure 9A,B). Model II has hydrogen bonds between the amidine protons and N3 of the internal adenines (Figure 9C). Model II is consistent with the berenil–d(TA)$_4$·d(TA)$_4$ structure presented by Pearl et al. (1987), where the central sequence, 5′A-T3′, is identical with ours. Since there is only a small change in the orientation of berenil molecule between models I and II, the berenil–DNA NOE contacts are very similar. One salient difference is that the model I predicts a strong contact between the amidine protons and H1′ of the external thymidine and of the internal guanosine, while model II predicts a strong contact between the amidine protons and H1′ of the internal adenosine. Unfortunately, the amidine–thymidine H1′ cross-peak could not be detected in the $1\bar{3}3\bar{1}$ pulse NOESY spectrum because the resonance of the thymidine H1′ (4.97 ppm) is very close to the H_2O signal. Since the amiding–guanosine H1′ and the amidine–adenosine H1′ cross-peaks are clearly absent from this NOESY spectrum (Figure 8), the two models remain indistinguishable on the basis of these predicted contacts.

A more quantitative comparison of the two models was carried out with the CORMA method. Differences between the observed and calculated NOE cross-peak intensities for the drug–DNA contacts of each model are summarized in Table III as the root mean square (RMS) values. The smaller RMS values for model II at mixing times of both 150 and 250 ms suggest that berenil may preferentially interact with the oligonucleotide by hydrogen bonding its amidine protons with the internal N3 of adenine. In both models, the diazoamino proton projects out of the minor groove and is not protected from exchange with solvent. This would explain why the diazoamino proton was not observed by NMR.

The H6 of both thymines and the H8 of the internal guanine showed weak NOE contacts with the berenil aromatic protons. These DNA protons, located in the major groove, are 5–7 Å from the berenil aromatic protons in both models described above, suggesting the possibility that these are indirect NOE contacts arising from spin diffusion.

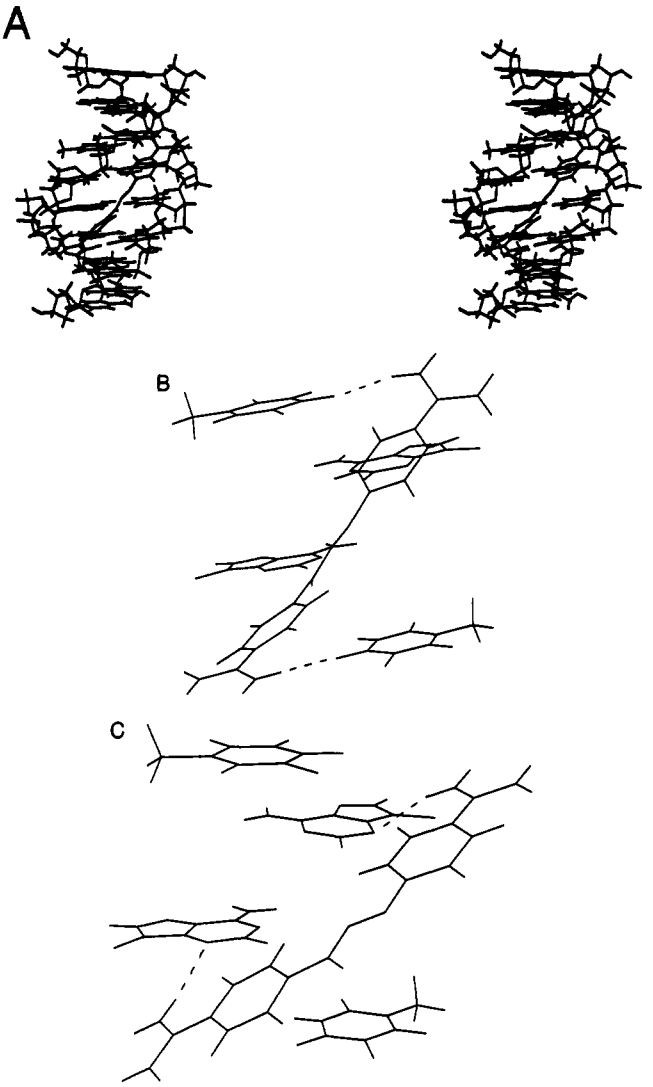

FIGURE 9: Stereoview of the berenil–d(GCAATTGC)$_2$ complex in model I with the hydrogen bond between berenil amidine protons and O2 of the external thymines (A). Simplified view of model I (B) and model II (C) to show the hydrogen bonding interactions and orientation of berenil with respect to the four AT base pairs. These hand-docked models were displayed with the molecular interactive graphics program MIDAS.

Table III: CORMA Analysis of Observed and Calculated NOESY Intensities (See Materials and Methods for Details)

mixing time (ms)	model	RMS value
150	I	0.047
150	II	0.023
250	I	0.032
250	II	0.019

CONCLUSIONS

This study represents the first attempt to determine the solution structure of both $d(GCAATTGC)_2$ and its complex with berenil by NMR spectroscopy. Data presented above for the oligonucleotide both alone and complexed with berenil demonstrate that the duplex is in a B conformation. NOE experiments provide evidence for binding of the drug in the minor groove of the oligonucleotide at the AATT sequence. Molecular models for this drug-DNA interaction that are consistent with our NMR data were generated on a computer graphics system and analyzed by CORMA. We are currently extending the graphical analysis of this system by carrying out energy minimization calculations.

ACKNOWLEDGMENTS

We are indebted to Dr. S. Neidle, Institute of Cancer Research, Sutton, Surrey, U.K., for providing us with the coordinates of berenil for the computer graphics and to Prof. T. L. James for making his CORMA computer program available. It also is a pleasure to acknowledge the Computer Graphics Laboratory at UCSF, Prof. Robert Langridge, Director.

REFERENCES

Braithwaite, A. W., & Baguley, B. C. (1980) *Biochemistry 19*, 1101-1106.
Ferrin, T. E., & Langridge, R. (1980) *Comput. Graphics 13*, 320.
Genest, D., Mazeau, K., & Ptak, M. (1987) *J. Biomol. Struct. Dyn. 5*, 67-78.
Gresh, N., & Pullman, B. (1984) *Mol. Pharmacol. 25*, 452-458.
Hore, P. J. (1983) *J. Magn. Reson. 55*, 283-300.
Keepers, J., & James, T. L. (1984) *J. Magn. Reson. 57*, 404-426.
Klevit, R. E., Wemmer, D. E., & Reid, B. R. (1986) *Biochemistry 25*, 3296-3303.
Kopka, M. L., Yoon, C., Goodsell, D., Pjura, P., & Dickerson, R. E. (1985a) *J. Mol. Biol. 183*, 553-563.
Kopka, M. L., Yoon, C., Goodsell, D., Pjura, P., & Dickerson, R. E. (1985b) *Proc. Natl. Acad. Sci. U.S.A. 82*, 1376-1380.
Landy, S. B., & Rao, B. D. N. (1989) *J. Magn. Reson. 81*, 371-377.
Langridge, R., Ferrin, T. E., Kuntz, I. D., & Connolly, M. L. (1981) *Science 211*, 661.
Leupin, W., Chazin, W. J., Hybert, S., Denny, W. A., & Wuthrich, K. (1986) *Biochemistry 25*, 5902-5910.
Newton, B. A. (1967) *Biochem. J. 105*, 50-51.
Patel, D. J., & Shapiro, L. (1986) *J. Biol. Chem. 261*, 1230-1240.
Pearl, L. H., Skelly, J. V., Hudson, B. D., & Neidle, S. (1987) *Nucleic Acids Res. 15*, 3469-3478.
Portugal, J., & Waring, M. J. (1987) *Eur. J. Biochem. 167*, 281-289.
Sanders, J. K. M., & Hunter, B. K. (1988) in *Modern NMR Spectroscopy*, pp 208-214, Oxford University Press, Oxford, New York, and Toronto.
Waring, M. (1970) *J. Mol. Biol. 54*, 247-279.
Wuthrich, K. (1986) in *NMR of Proteins and Nucleic Acids*, pp 203-223, Wiley-Interscience Publication, New York, Chichester, Brisbane, Toronto, and Singapore.

Quaternary Interactions in Eye Lens β-Crystallins: Basic and Acidic Subunits of β-Crystallins Favor Heterologous Association†

C. Slingsby* and O. A. Bateman
Laboratory of Molecular Biology, Department of Crystallography, Birkbeck College, Malet Street, London, WC1E 7HX U.K.
Received February 14, 1990; Revised Manuscript Received April 11, 1990

ABSTRACT: β-Crystallins are complex eye lens proteins made up of several related basic and acidic subunits that combine to form differently sized oligomers each displaying extensive polydispersity. As the sequences are homologous to the X-ray-determined bilobal structure of γ-crystallin, β-subunits are visualized as having a similar structure with additional N- and C-terminal extensions. Two basic (βB2 and βB3) and two acidic (βA3 and βA4) subunits have been isolated in deaggregating media, refolded, and reassociated in various combinations to determine which components favor dimers or higher oligomers. Homopolymers were compared with βB2 homodimer in terms of charge, using Mono Q fast protein liquid chromatography, and size, using Superose 12 chromatography. Heterooligomeric formations were monitored by their intermediate charge properties compared with homooligomers. βB2 associates with either βB3- or βA4-forming heterodimers whereas a larger oligomer is formed with βA3. Naturally occurring β-crystallin oligomers were analyzed by Mono Q chromatography and PhastGel electrophoresis. Whereas βB2, βB3, and βA4 can each be reassociated to homodimers, βA4 dimers are not found in native β-crystallins. βB2-βA3 is a major component of intermediate-sized βL_1-crystallin and is absent from dimeric βL_2-crystallin. It is suggested that the pH dependence of the size of βL_1-crystallin is due to a dimer to tetramer equilibrium. By following dimer interactions using Superose 12 chromatography, βB2-βA4 was shown to interact with βB2-βA3. A model of β-crystallin structure is proposed based on β-subunits forming dimers with the next level of organization requiring an acidic subunit, βA3, with a long N-terminal extension.

Refractive index is the fundamental property which determines the focal power of lenses. In animal lenses, heterogeneous populations of globular oligomeric and monomeric crystallins are packed together inside cells (Harding & Crabbe, 1984; Wistow & Piatigorsky, 1988), forming protein concentration gradients from which optical characteristics are

† This work was supported by the Medical Research Council (London).

0006-2960/90/0429-6592$02.50/0